CSI-based NOMA for Integrated Sensing and Communication

CSI-based NOMA for Integrated Sensing and Communication

Ebubekir Memisoglu, Halise Türkmen, Basak Ak Ozbakis, and Hüseyin Arslan, *Fellow, IEEE*

Abstract—Integrated sensing and communication (ISAC) is a key enabler of fifth-generation and beyond networks and a multitude of futuristic applications. However, the coexistence, scheduling and scarcity issues due to additional sensing signals are valid concerns. If a communicating device also requires sensing, it can use its communication signal for sensing. But if a non-communicating device requires sensing, the additional sensing signals will cause extra traffic in the network. Thus, in this letter, a novel integrated sensing and communication with iterative channel estimation (ISAC-ICE) method is proposed to provide spectral efficiency while maintaining sensing and communication performance. The simulation results and complexity analysis demonstrate that the proposed method with a linearithmic complexity enables non-orthogonal multiple accessing (NOMA) of ISAC.

Index Terms—Integrated sensing and communication, non-orthogonal multiple access (NOMA), channel state information (CSI), iterative channel estimation.

I. Introduction

Integrated sensing and communications (ISAC) systems, i.e., wireless-capable systems which can share and/or coordinate resources to perform both sensing and communication, have garnered a lot of attention from the industry and academia, and are envisioned to be the second functionality of future wireless networks [1]. As such, leading wireless communication standardization entities, such as the wireless fidelity (Wi-Fi) Alliance and 3rd Generation Partnership Project (3GPP), have initiated research in to standardizing and enhancing sensing within wireless networks [2], [3]. However, the inclusion of wireless sensing into communication networks is not straightforward. The increase in wireless sensing applications, and consequently signals, will inevitably increase the network traffic, causing coexistence, scheduling and interference issues [4].

One approach is to mitigate this problem is to design a waveform such that both the communication and sensing performance requirements are satisfied with the same signal. However, meeting these requirements results in trade-offs between sensing and communication performances [1]. Scheduling-based approaches are also present, where the focus is on isolating the sensing and communication signals in the time and/or frequency domains [5]. For example, TGbf, the task group responsible for incorporating sensing in Wi-Fi, has opted to transmit packets containing only training fields, or

pilots, for sensing, using the same channel access mechanisms as the communication packets [6]. This means that the sensing and communication transmissions will compete for transmission opportunity, which will degrade the communication capacity, especially if many sensing users (SUs) are present in the vicinity. As such, these methods are not resource efficient.

A different, more recent approach is non-orthogonal multiple access (NOMA)-ISAC. Here, the sensing signals and communication signals are overlapped, either at the transmitter or in the channel, and separated at the receiver(s). One such example is NOMA with two different waveforms, as in [7], where an orthogonal frequency division multiplexing (OFDM) and frequency modulated continuous wave (FMCW) signal are overlapped. Other works either assume the sensing signal to be known and perfectly removable [8] or assume the sensing signal as a virtual communication signal and apply successive interference cancellation (SIC) [9]. In the former, a radar echo is overlapped with an uplink signal at the ISAC base station. In the latter, a sensing signal and a communication signal are transmitted to the user equipment (UE), which removes the sensing signal and sends feedback information. Their aim is to jointly optimize the sensing and communication beams such that the communication performance is satisfied while the nearby objects are detected by the base station (BS). Both of these works consider beamforming communication and, as with most power domain NOMA works, assume perfect channel knowledge of the communicating UEs. This assumption is unrealistic, however, as the devices would have to do channel estimation with a non-NOMA signal beforehand. Furthermore, satisfying and maintaining the power difference criteria required to apply SIC is difficult, more so in a mobile target and/or UE scenario. All [7]–[9] assume that the sensing and communication signals are transmitted by the same device; i.e., sensing is done by a device which is also communicating, and ignore scenarios where the sensing and communication signals are transmitted by two different devices.

In light of this, this paper proposes a novel NOMA-ISAC scheme for channel state information (CSI)-based sensing where one device is a communicating user (CU) and the other is a SU. The transmitted OFDM signals are the random communication signal and known sensing signal, and their subcarriers are fully overlapped at the receiver, where iterative channel estimation is applied. Compared to the conventional orthogonal ISAC (CO-ISAC) systems, where the sensing and communication signals are separated in time or frequency domains, the proposed system, ISAC with iterative channel estimation (ISAC-ICE) enables sharing these resources and can attain a satisfactory bit error rate (BER) and mean squared error (MSE) for communication and sensing performance, respectively. Thus, the spectral efficiency will be improved.
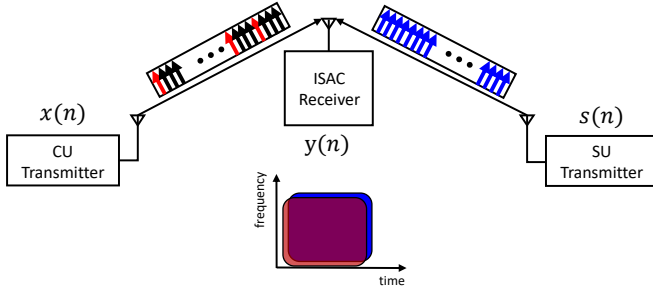
Fig. 1. The system model of CSI-based NOMA scheme.

II. SYSTEM MODEL

The system model comprises of two separate and independent single-antenna CU and SU transmitters, which simultaneously transmit their signals over a wireless channel to a single-antenna ISAC receiver. The OFDM communication symbol consists of pilot and data subcarriers, and the OFDM sensing symbol contains sensing sequences. As they are transmitted simultaneously, the communication and sensing transmissions occupy the same time and frequency resources. The entirety of the system model is depicted in Fig. 1. Here, the black, red, and blue arrows in the rectangles represent the data, pilot, and sensing subcarriers, respectively, over a bandwidth. The overlapping of communication and sensing signals is illustrated with the red and blue rectangles respectively in the time-frequency plane. For the parallel transmission, it is assumed that communication and sensing transmitters are perfectly synchronized in time and frequency domains with the receiver.

The discrete time-domain OFDM symbol is generated at the CU transmitter as

$$x(n) = \frac{1}{\sqrt{N}} \sum_{k=0}^{N-1} X(k) e^{j2\pi k(n-N_{cp})/N}, \tag{1}$$
$$n = 0, 1, \ldots, N + N_{cp} - 1,$$

where $X(k)$ denotes the data and pilot symbols, and N_{cp} is the cyclic prefix (CP) length. Here, the data and pilot indices are denoted by k_d and k_p, respectively, where $X(k_d)$ has an average unit power and $X(k_p) \in \{-1, 1\}$. Similarly, the sensing symbol at the SU transmitter is generated as

$$s(n) = \frac{1}{\sqrt{N}} \sum_{k=0}^{N-1} S(k) e^{j2\pi k(n-N_{cp})/N}, \quad S(k) \in \{-1, 1\}. \tag{2}$$

Then, digital-to-analog conversion is performed and these signals are separately transmitted through the wireless channel. Here, although the same N_{cp} is used for both the communication and sensing symbol generation, different N_{cp} values can also be used, as long as they are larger that the maximum excess delay of both the communication and sensing channels.

At the ISAC receiver, first analog-to-digital conversion is performed to obtain $y(n)$, followed by the removal of the CP and the discrete Fourier transform (DFT) operation. Finally, the received frequency domain signal can be written as

$$Y(k) = \sqrt{\rho_c} H_c(k) X(k) + \sqrt{\rho_s} H_s(k) S(k) + W(k), \tag{3}$$

where ρ_c, ρ_s, $H_c(k)$, $H_s(k)$, $W(k)$ denote the received signal powers of communication and sensing signals, Rayleigh fading channel samples with the distribution of $\mathcal{CN}(0, 1)$, and noise sample with the distribution of $\mathcal{CN}(0, \sigma_0^2)$, respectively. Then, an iterative channel estimation for the communication and sensing channels is performed. After the equalization with the estimated communication channel, the received symbols are demodulated.

III. ITERATIVE CHANNEL ESTIMATION

In conventional channel estimation in OFDM systems, the pilot or known symbols are used to estimate the channel. Then, the obtained CSI is used for demodulating the data symbols or sensing. In the NOMA-ISAC scenario, the signals are fully overlapped in the time and frequency domain, therefore the signals are not separable and conventional channel estimation is no longer feasible. Here, for a good signal separability, an iterative channel estimation algorithm of the communication and sensing channels is developed in this section.

First, the received frequency domain signal in (3) is required. Since $\mathbf{S}$ is known at the ISAC receiver, the sensing CSI estimation can be obtained by using a least-square (LS) or minimum-mean-square-error (MMSE) estimator [10]. In this paper, the LS estimator is utilized, but MMSE can also be used. The sensing CSI with LS estimator for the i-th iteration is found as

$$\widetilde{\mathbf{H}}_s^{(i)} = \mathbf{S}^{-1} \mathbf{Y}_s^{(i-1)}, \tag{4}$$

where $\mathbf{Y}_s^{(i-1)}$ is the received sensing signal with $\mathbf{Y}_s^{(0)} = \mathbf{Y}$ for $i = 1, 2, \ldots, I$. Here, I represents the total number of the iterations in ISAC-ICE. To improve the estimation performance, the DFT-based channel estimation is applied to $\widetilde{\mathbf{H}}_s^{(i)}$ as below,

$$\widetilde{h}_s^{(i)}(n) = \frac{1}{\sqrt{N}} \sum_{k=0}^{N-1} \widetilde{H}_s^{(i)}(k) e^{j2\pi kn/N}, \tag{5}$$

$$\widetilde{H}_{s,DFT}^{(i)}(k) = \sqrt{N} \sum_{n=0}^{N_{cp}-1} \widetilde{h}_s^{(i)}(n) e^{-j2\pi nk/N}. \tag{6}$$

Then, the estimated sensing signal is subtracted from (3) as

$$\mathbf{Y}_c^{(i)} = \mathbf{Y} - \mathbf{S}\widetilde{\mathbf{H}}_{s,DFT}^{(i)}. \tag{7}$$

The effects of sensing signal on communication signal are partially removed after this subtraction. Thereafter, the conventional processes of OFDM at the receiver are done to detect the transmitted data symbols. For the communication channel estimation of $\widetilde{H}_c^{(i)}(k_p)$, the subcarriers of $Y_c^{(i)}(k_p)$ are divided by $X(k_p)$ as $\widetilde{H}_c^{(i)}(k_p) = X(k_p)^{-1} Y_c^{(i)}(k_p)$, and fitted with a cubic spline to obtain $\widetilde{H}_c^{(i)}(k)$. Then, the DFT-based channel estimation is applied to obtain $\widetilde{\mathbf{H}}_{c,DFT}^{(i)}$, as in (5) and (6). Next, the channel equalization is performed as

$$\overline{\mathbf{Y}}_c^{(i)} = \widetilde{\mathbf{H}}_{c,DFT}^{(i)}{}^{-1} \mathbf{Y}_c^{(i)}. \tag{8}$$

Then, $\overline{Y}_c^{(i)}(k_d)$ is demodulated to obtain $\widetilde{X}^{(i)}(k_d)$. Since $X(k_p)$ is known and $\widetilde{X}^{(i)}(k_d)$ is detected at the receiver, a

Algorithm 1 Proposed iterative CSI estimation.

1: Define N, k_d, and k_p
2: Obtain $\mathbf{Y}$
3: Set $\mathbf{Y}^{(0)} = \mathbf{Y}$
4: **for** $i = 1$ **to** I **do**
5:     Obtain $\widetilde{\mathbf{H}}_s^{(i)}$
6:     Obtain $\widetilde{\mathbf{H}}_{s,DFT}^{(i)}$
7:     Obtain $\mathbf{Y}_c^{(i)}$
8:     Obtain $\overline{\mathbf{Y}}_c^{(i)}$ and $\widetilde{\mathbf{H}}_{c,DFT}^{(i)}$
9:     Obtain $\widetilde{\mathbf{H}}_{c,DD}^{(i)}$
10:    Obtain $\mathbf{Y}_s^{(i)}$
11: **end for**
12: Find $\overline{\mathbf{Y}}_c^{(I)}$, $\widetilde{\mathbf{H}}_{c,DFT}^{(I)}$, and $\widetilde{\mathbf{H}}_{s,DFT}^{(I)}$

decision-directed (DD) channel estimation can be performed to improve $\widetilde{H}_{c,DFT}^{(i)}(k)$ as

$$\widetilde{\mathbf{H}}_{c,DD}^{(i)} = \left[\widetilde{\mathbf{X}}^{(i)}\right]^{-1} \overline{\mathbf{Y}}_c^{(i)}. \qquad (9)$$

Intuitively, the accuracy of $\widetilde{\mathbf{H}}_{c,DD}^{(i)}$ increases when the detection of $\widetilde{X}^{(i)}(k_d)$ has lower error rate.

Using the superior estimated channel, $\widetilde{\mathbf{H}}_{c,DD}^{(i)}$, the updated sensing signal can be obtained by subtracting the estimated communication signal from the received signal as

$$\mathbf{Y}_s^{(i)} = \mathbf{Y} - \widetilde{\mathbf{H}}_{c,DD}^{(i)} \widetilde{\mathbf{X}}^{(i)}. \qquad (10)$$

Afterwards, (4), (5), (6), (7), (8), and (9) are repeated until the maximum iteration value, I, is reached. The steps of the iterative CSI estimation at the ISAC receiver are summarized in Algorithm 1.

For the computational complexity analysis, the real additions and multiplications over an OFDM duration are considered at the receiver side. For $\widetilde{\mathbf{H}}_s^{(i)}$, $\widetilde{\mathbf{H}}_c^{(i)}$, $\widetilde{\mathbf{H}}_{c,DD}^{(i)}$, and $\overline{\mathbf{Y}}_c^{(i)}$, $2N$ real multiplications are required for one iteration. For $\mathbf{Y}_c^{(i)}$ and $\mathbf{Y}_s^{(i)}$, $2N$ real additions and multiplications are required for one iteration. Since fast Fourier transform has the complexity of $(3N \log_2 N - 3N + 4)$ real additions and $(N \log_2 N - 3N + 4)$ real multiplications [11], the processes to obtain $\widetilde{\mathbf{H}}_{s,DFT}^{(i)}$ and $\widetilde{\mathbf{H}}_{c,DFT}^{(i)}$ have $4(3N \log_2 N - 3N + 4)$ real additions and $4(N \log_2 N - 3N + 4)$ real multiplications in total for one iteration. In CO-ISAC, where the channel estimation is done separately for both functionalities, $(12N \log_2 N - 12N + 16)$ real additions and $(4N \log_2 N - 6N + 16)$ real multiplications are required to obtain $\widetilde{\mathbf{H}}_s^{(1)}$, $\widetilde{\mathbf{H}}_c^{(1)}$, $\widetilde{\mathbf{H}}_{s,DFT}^{(1)}$, $\widetilde{\mathbf{H}}_{c,DFT}^{(1)}$, and $\overline{\mathbf{Y}}_c^{(1)}$. Therefore, the additional computational complexity of ISAC-ICE for I iterations can be written as

$$I(12N \log_2 N - 8N + 16) - (12N \log_2 N - 12N + 16), \quad (11)$$

$$I(4N \log_2 N + 16) - (4N \log_2 N - 6N + 16), \qquad (12)$$

for real additions and multiplications, respectively.

IV. SIMULATION RESULTS

In this section, the BER, MSE, and spectral efficiency performances of are analyzed via Monte Carlo simulations. In the proposed method, the time and frequency resources are equally
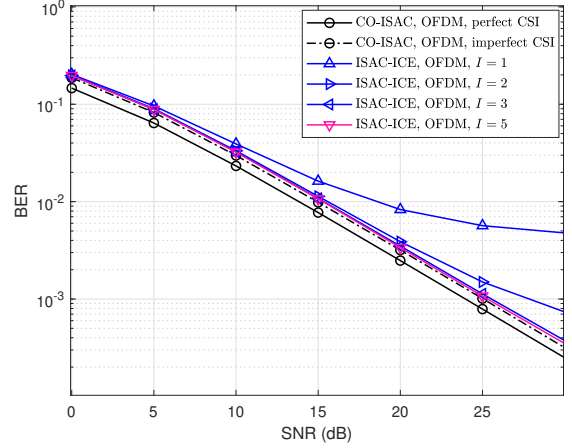
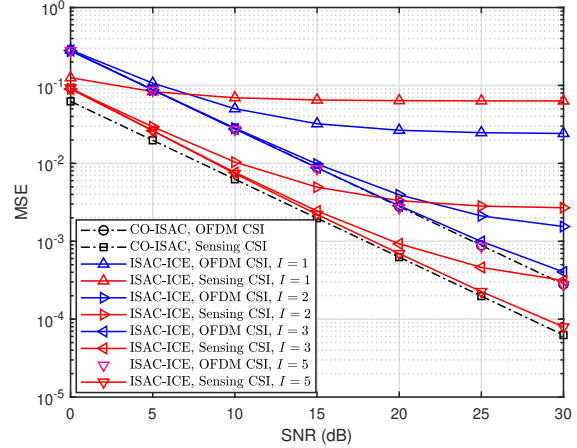Fig. 2. The BER performance of ISAC-ICE for different I values.

Fig. 3. The MSE performance of the OFDM and sensing CSI estimation for different I values.

shared between communication and sensing systems. A binary phase-shift keying (BPSK) modulated signal is used with $1/4$ pilot ratio and signal parameters $N = 256$, $N_{cp} = 16$, and $\rho_c = \rho_s = 1$ for the simulations. For the channel, a 8 tap frequency selective Rayleigh fading channel is considered.

The BER performance of ISAC-ICE is compared with CO-ISAC with perfect and imperfect CSI cases in Fig. 2. As seen from the figure, ISAC-ICE has a significant loss; however, as the I value increases the BER performance improves. The improvement is not proportional with the increase of I, and first iterations provide the most significant improvement. The lower bound performance of the proposed method is taken as the CO-ISAC performance, and can be achieved with $I = 3$ iterations. As I is further increased, it can be seen that there is no significant change in BER performance while the overall computational complexity increases.

The MSE performance of ISAC-ICE compared to CO-ISAC is given in Fig. 3. The MSE is calculated by taking the expected value of $\left(\mathbf{H}_c - \widetilde{\mathbf{H}}_{c,DFT}^{(I)}\right)^2$ and $\left(\mathbf{H}_s - \widetilde{\mathbf{H}}_{s,DFT}^{(I)}\right)^2$ for the OFDM and sensing CSIs, respectively. In CO-ISAC, the OFDM and sensing CSIs have the best performance, therefore
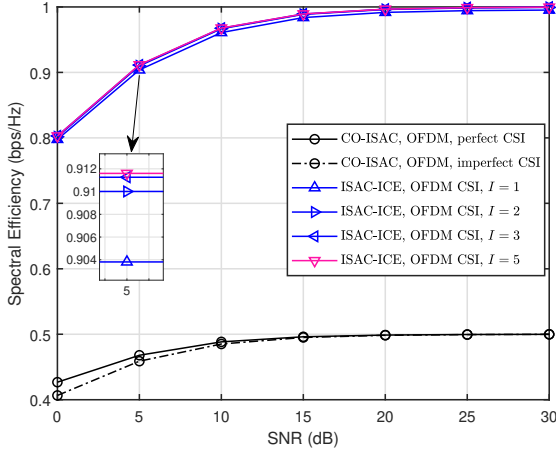
Fig. 4. The spectral efficiency of ISAC-ICE for different I values.

TABLE I
COMPUTATIONAL COMPLEXITY COMPARISON

		Additions	Multiplications
CO-ISAC		21520	6672
ISAC-ICE	$I = 1$	22544	8208
	$I = 2$	45088	16416
	$I = 3$	67632	24624
	$I = 5$	112720	41040

$I = 3$ iterations, which results in an additional 46112 real additions and 17952 real multiplications, as calculated using (11) and (12), respectively. Similarly, to achieve near CO-ISAC performance in MSE for sensing CSI, at least $I = 5$ iterations are required. In this case, ISAC-ICE requires an additional 91200 real additions and 34368 real multiplications. Although the ISAC-ICE with $I = 1$ has a similar complexity to CO-ISAC, it has significant losses in the BER and MSE performances. Therefore, a better spectral efficiency can be obtained with a linear increase in the complexity.

V. CONCLUSION

In this letter, a novel iterative channel estimation method, ISAC-ICE, has been proposed to separate the communication and sensing signals in a NOMA case. The results demonstrate that ISAC-ICE can achieve a similar BER and MSE performance to CO-ISAC with a better spectral efficiency. As a trade-off, ISAC-ICE increases the computational complexity linearly with the number of iterations. Since spectral efficiency losses due to CO-ISAC are eliminated by ISAC-ICE, the sensing requirements can be met without degrading communication performance. For the future work, the asynchronous transmission of communication and sensing users will be investigated.

REFERENCES

[1] Z. Wei *et al.*, "Toward multi-functional 6G wireless networks: Integrating sensing, communication, and security," *IEEE Commun. Mag.*, vol. 60, no. 4, pp. 65–71, Apr. 2022.
[2] C. Silva, "802.11 SENS SG proposed PAR," *IEEE 802.11-19/2103r12*, Aug. 2020.
[3] 3GPP SP 220717, "Revised SID on integrated sensing and communication," Jun. 2022.
[4] L. Zheng, M. Lops, Y. C. Eldar, and X. Wang, "Radar and communication coexistence: An overview: A review of recent methods," *IEEE Signal Process. Mag.*, vol. 36, no. 5, pp. 85–99, Sep. 2019.
[5] J. Qian *et al.*, "Radar and communication spectral sharing under multiple spectral compatibility constraints," *IEEE Wireless Commun. Lett.*, vol. 11, no. 10, pp. 2120–2124, Oct. 2022.
[6] R. Du *et al.*, "An overview on IEEE 802.11bf: WLAN sensing," Jul. 2022. [Online]. Available: https://arxiv.org/abs/2207.04859
[7] M. Mert Şahin and H. Arslan, "Multi-functional coexistence of radar-sensing and communication waveforms," in *Proc. IEEE 92nd Veh. Technol. Conf. (VTC2020-Fall)*, Nov. 2020, pp. 1–5.
[8] C. Ouyang *et al.*, "On the performance of uplink ISAC systems," *IEEE Commun. Lett.*, vol. 26, no. 8, pp. 1769–1773, Aug. 2022.
[9] Z. Wang, Y. Liu, X. Mu, and Z. Ding, "NOMA inspired interference cancellation for integrated sensing and communication," in *Proc. IEEE Int. Conf. Commun.*, May 2022, pp. 3154–3159.
[10] Y. S. Cho, J. Kim, W. Y. Yang, and C. G. Kang, *MIMO-OFDM wireless communications with MATLAB*. John Wiley & Sons, 2010.
[11] H. V. Sorensen, M. Heideman, and C. Burrus, "On computing the split-radix FFT," *IEEE Trans. Acoust., Speech, and Signal Process.*, vol. 34, no. 1, pp. 152–156, Feb. 1986.

it will be the lower bound for ISAC-ICE. As expected, ISAC-ICE has worse MSE performance due to NOMA and there is a significant loss in MSE when $I = 1$. However, as I increases, this loss can be compensated because after each iteration, more accurate CSIs are obtained and used in the following iteration. With $I = 5$ iterations, ISAC-ICE can achieve a similar MSE performance compared to CO-ISAC CSIs. It is important to point out that for the sensing signal, although for CO-ISAC there is less error in the channel estimation due to the all the subcarriers being pilots, in ISAC-ICE more iterations are required to approach the lower bound than for the communication signal. This is because the channel estimation for the sensing signal is done first, meaning that there will always be more interference from the communication signal to the sensing signal. Meanwhile, for the channel estimation of the communication signal, the sensing signal is removed, as in (7). For $I = 1$, the performance is the worst because the interference from the communication signal is not removed at all. For a higher number of iterations, channel estimation for sensing is done on the updated sensing signal, $\mathbf{Y}_s^{(i)}$, which is found by removing the communication signal interference, as in (10).

In ISAC-ICE, a similar BER and MSE performance compared to the case of CO-ISAC can be achieved. Consequently, due to the NOMA scheme, the spectral efficiency of communication systems is improved, as seen in Fig. 4. The spectral efficiency is calculated as the division of the number of transmitted correct bits over a bandwidth by the total time duration. Since the resources are equally and orthogonally shared in CO-ISAC, ISAC-ICE provides approximately double the spectral efficiency while having a similar OFDM and sensing CSI performance.

The improved spectral efficiency in ISAC-ICE comes at the cost of increased computational complexity at the receiver. This can be seen in Table 1, where the total computational complexities for CO-ISAC and ISAC-ICE is given for $I = [1, 2, 3, 5]$. The overall complexity of ISAC-ICE is $\mathcal{O}(IN \log_2 N)$ and linearly increases with I. To achieve near CO-ISAC performance in BER, ISAC-ICE requires at least